

## Experimental verification of optimal strain gage locations for the accurate determination of stress intensity factors

H. Sarangi<sup>1</sup>, K.S.R.K. Murthy<sup>2\*</sup>, D. Chakraborty<sup>2</sup>

<sup>1</sup> Research Scholar, Department of Mechanical Engineering, IIT Guwahati, Guwahati 781039, India

<sup>2</sup> Faculty of Department of Mechanical Engineering, IIT Guwahati, Guwahati 781039, India

\* Corresponding author: ksrkm@iitg.ernet.in

---

**Abstract** In the present investigation experimental verification of optimal strain gage locations and their importance in accurate determination of mode I stress intensity factors (SIFs) using Dally and Sanford's single strain gage technique (DS technique) has been carried out. The results of the present experimental study are also used to substantiate the efficacy of the methodology for determination of maximum permissible strain gage radial location proposed earlier by the same authors for locating the optimal strain gage locations. Experiments have been conducted using an edge cracked plate made of Polymethylmethacrylate. Results clearly demonstrate that very accurate values of mode I SIFs can be determined if the strain gages are placed at the optimal locations. On the other hand, the experimental results also show that the mode I SIFs obtained using strain gages placed at non-optimal locations contain significant and unacceptable errors. The results of the present investigation clearly confirm the importance of knowing the maximum permissible strain gage radial location corresponding to an experimental specimen before conducting experiment for determination of mode I SIF using the DS strain gage technique.

**Keywords** Stress intensity factor, Strain gage, Gage location, Optimal

---

### 1. Introduction

Stress intensity factor is an important parameter in linear elastic fracture mechanics. Strain gage based experimental techniques for the determination of stress intensity factors (SIFs) are equally powerful in experimental fracture mechanics as other methods such as photoelasticity, caustics and moiré interferometry etc. [1]. For many years, local yielding, high strain gradients, strain gradient effects due to finite size of gages and three dimensional effects near the crack tip were the major problems associated with the application of strain gage techniques for accurate determination of SIFs.

Dally and Sanford [2] was the first to propose a practically feasible single strain gage technique to overcome most of the above mentioned difficulties. Their technique (DS technique) is theoretically well supported and is proposed for determination of mode I SIF,  $K_I$  of two dimensional single ended cracked configurations made of isotropic materials. Many different strain gage techniques for determination of SIFs under different situations have been proposed subsequently by various researchers [3-6]. Among the available strain gage techniques for the determination of  $K_I$ , DS technique [2] has been more widely employed [7-11] in different contexts.

Referring to Fig. 1, it is evident that in order to obtain accurate values of the SIFs, it is very important to decide strain gage angular location and orientation (defined by  $\theta$  and  $\alpha$ ) with

respect to the crack axis and radial location ( $r$ ) from the crack tip to the center of the gage. The most difficult and challenging problem is in deciding the appropriate radial distance ( $r$ ) for each of the selected number of strain gages for the measurement of  $K_I$ . The radial location of strain gages  $r$  is restricted by plasticity effects, three dimensional (3D) effects, strain gradients and the analytical strain series used. To avoid plasticity, strain gradient and 3D effects strain gages should not be placed very close to the crack-tip [2, 6]. On the other hand, strain gages placed at a large distance from the crack-tip may not be represented by the selected strain series. Thus, the radial location of a strain gage from the crack-tip is one of the most important parameters required to be known apriori for accurate determination of the SIFs using strain gage techniques.

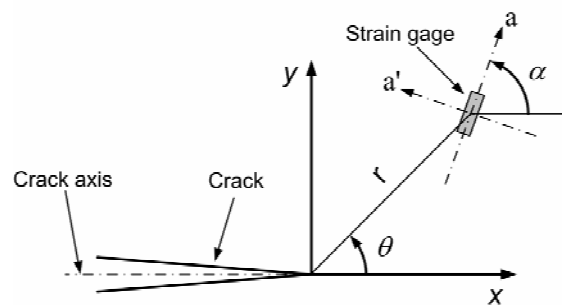


Figure 1. Location of a strain gage from the crack tip

Literature review on strain gage techniques [2-11] show that until recently, no recommendation, or no methodology, or no solution in any form is available for selection of appropriate radial locations ( $r$ ) for the strain gage in the DS technique despite its popularity. As a consequence, the issue of valid strain gage locations for determination of SIFs using the DS technique remained as an open problem for long time [1].

Recently, Sarangi et al. [12, 13] proposed an approach for determination of optimal or valid radial locations for single strain gage in the DS technique. A methodology based on the finite element analysis (FEA) supported by theoretical foundations has been presented by them [12, 13] for the first time for obtaining the optimal radial gage locations. They defined a parameter  $r_{max}$  which is the upper bound on the radial location for the strain gage which in turn can be used for locating the optimal or valid radial locations for strain gages. Further details on  $r_{max}$  can be found in Refs. [12, 13].

No experimental investigation is reported till date to demonstrate the existence of optimal radial locations for strain gages and their usefulness in accurate determination of mode I SIFs using the DS technique. Thus, the objectives of the present investigation are (a) experimental verification of the optimal strain gage locations obtained using the approach proposed by Sarangi et al. [12, 13], (b) to show the usefulness of these locations in obtaining accurate mode I SIFs of cracked configurations using the DS technique and (c) to substantiate the usefulness of methodology for

determination of maximum permissible strain gage radial location  $r_{\max}$  proposed by Sarangi et al. [12, 13] for locating the optimal strain gage locations.

## 2. Theoretical Background

A very brief theoretical background on the DS technique [2] and determination of optimal strain gage locations for this technique proposed by Sarangi et al. [12, 13] is presented in this section. It can be shown that the strain  $\varepsilon_{aa}$  (Fig. 1) at a point  $P$  (defined by  $r$  and  $\theta$ ) in the direction of an arbitrary angle  $\alpha$  (with respect to the crack axis) for plane stress conditions is given by [2, 12, 13]

$$2G\varepsilon_{aa} = A_0 r^{-1/2} \left[ \kappa \cos \frac{\theta}{2} - \frac{1}{2} \sin \theta \sin \frac{3\theta}{2} \cos 2\alpha + \frac{1}{2} \sin \theta \cos \frac{3\theta}{2} \sin 2\alpha \right] + A_1 r^{1/2} \cos \frac{\theta}{2} \left[ \kappa + \sin^2 \frac{\theta}{2} \cos 2\alpha - \frac{1}{2} \sin \theta \sin 2\alpha \right] + B_0 (\kappa + \cos 2\alpha) \quad (1)$$

where  $\kappa = (1-\nu)/(1+\nu)$  and  $A_0$ ,  $A_1$  and  $B_0$  are unknown coefficients. Eq. (1) is obtained using the three parameter representation of the strain field (in terms of coefficients  $A_0$ ,  $A_1$  and  $B_0$ ) around the crack tip. Using the definition of  $K_I$  it can be shown that the singular coefficient  $A_0$  is related to the mode I SIF  $K_I$  as

$$K_I = \sqrt{2\pi} A_0 \quad (2)$$

The coefficient of  $B_0$  term in Eq. (1) can also be eliminated by selecting the angle  $\alpha$  such that

$$\cos 2\alpha = -\kappa = -\frac{1-\nu}{1+\nu} \quad (3)$$

Similarly coefficient of  $A_1$  can also be made zero if the angle  $\theta$  is selected as

$$\tan \frac{\theta}{2} = -\cot 2\alpha \quad (4)$$

With  $\alpha$  and  $\theta$  as defined by Eqs. (3) and (4), the simplified form of Eq. (1) is given by

$$2G\varepsilon_{aa} = \frac{K_I}{\sqrt{2\pi r}} \left[ \kappa \cos \frac{\theta}{2} - \frac{1}{2} \sin \theta \sin \frac{3\theta}{2} \cos 2\alpha + \frac{1}{2} \sin \theta \cos \frac{3\theta}{2} \sin 2\alpha \right] \quad (5)$$

Thus, by placing a single strain gage (Fig. 1) with  $\alpha$  and  $\theta$  as defined by Eqs. (3) and (4) the strain  $\varepsilon_{aa}$  can be measured and  $K_I$  can be determined using Eq. (5).

Using numerical and experimental studies [14, 15] it has been established that the 3D effects prevail up to a radial distance equal to half the thickness of the plate from the crack tip. Therefore, the minimum radial distance  $r_{\min}$  for strain measurements on the free surface should be greater than half the thickness of the plate [2]. As a consequence, the optimal or valid radial location  $r$  for a strain gage in DS technique can now be given as

$$r_{\min} \left( = \frac{\text{thickness of plate}}{2} \right) \leq r \leq r_{\max} \quad (6)$$

where the unknown parameter  $r_{\max}$  is defined as the maximum permissible radial distance for the strain gage or the extent of validity of Eq. (5) from the crack tip. It is clear that Eq. (5) can accurately describe the strain field in the given direction  $\theta$  only up to a radial distance  $r_{\max}$  from the crack tip and beyond this radial distance more number of coefficients other than  $A_0$ ,  $A_1$  and  $B_0$  are needed to represent the strain field. Clearly, with this definition of  $r_{\max}$ , any radial distance of strain gage satisfying the Eq. (6) is an optimal radial location. According to Sarangi et al. [12, 13], for a given configuration, applied load, Young's modulus  $E$  and Poisson's ratio  $\nu$  Eq. (5) can be simplified as,

$$\varepsilon_{aa} = \frac{C}{\sqrt{r}} \quad (7)$$

where  $C$  is a constant. Taking logarithm on both sides of Eq. (7)

$$\ln(\varepsilon_{aa}) = -\frac{1}{2} \ln(r) + \ln(C) \quad (8)$$

Clearly Eq. (8) is valid along the line given by Eq. (4) for  $r \leq r_{\max}$ . Thus a plot of Eq. (7) on log-log axes ( $\ln(\varepsilon_{aa})$  versus  $\ln(r)$ ) depicts a straight line of slope equals to  $-0.5$ , with an intercept of  $\ln(C)$ . Theoretically, the straight line property will break beyond  $r > r_{\max}$  as more than three parameters are needed in Eq. (1) to estimate the  $\varepsilon_{aa}$ . Using the straight line property exhibited by Eq. (8), the value of  $r_{\max}$  can be accurately estimated from the log-log plots of  $\varepsilon_{aa}$  and  $r$ . Other details on computation of  $r_{\max}$  can be found in Refs.[12, 13].

### 3. Experimental Verification

Present section describes experimental verification of optimal radial locations of strain gages obtained using the approach described in the previous section and their use in determination of accurate mode I SIFs. The following equations are employed for determination of normalized SIF

$K_I$

$$F_I = \frac{K_I}{\sigma\sqrt{\pi a}} \quad (9)$$

where  $\sigma$  is the nominal stress and  $a$  is the crack length and the % relative error in  $F_I$  is calculated as

$$\% \text{ Relative error} = \left( \frac{F_I^{\text{reference solution}} - F_I^{\text{experimental}}}{F_I^{\text{reference solution}}} \right) \times 100 \quad (10)$$

### 3.1 Details of experimental specimen

In the present experimental investigation, commercially available Polymethylmethacrylate (PMMA) has been used as the material for the test specimen. It is well known that PMMA is a homogeneous, isotropic and brittle material at room temperature [16]. The test specimen considered in the present investigation is straight edge cracked plate subjected to tensile loading as shown schematically in Fig. 2(a). The details of geometry and that of pre-crack are also shown in Fig. 2(a). Experiments have been conducted using an edge cracked plate having  $a/b$  ratio 0.493. The geometric and other details of the experimental specimen have been presented in Table 1. Fig. 2(b) shows actual specimen with strain gages mounted on the surface. Dimensions and loading conditions in the test specimen have been chosen so as to ensure plane stress conditions during the experiments. The elastic properties of PMMA sheet obtained from tensile tests have also been presented in Table 1.

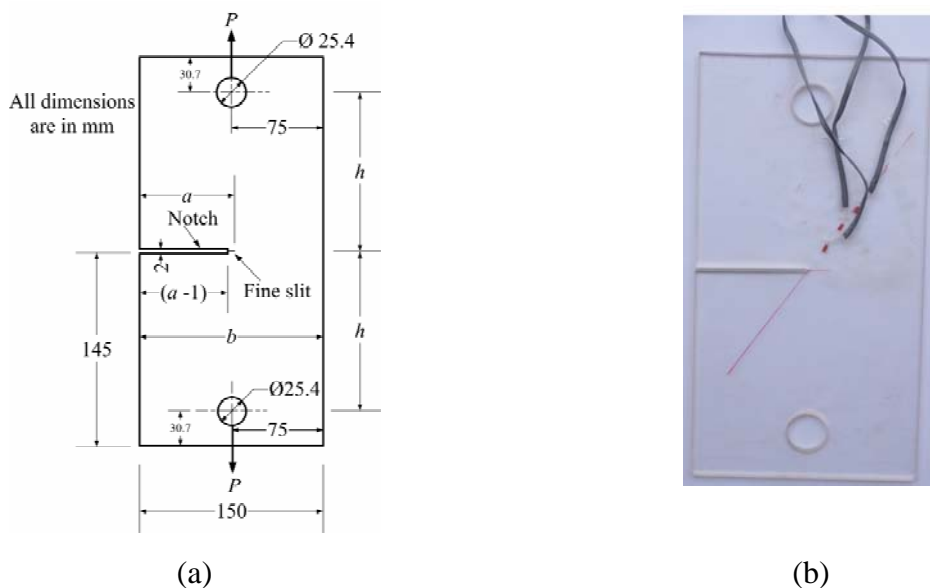


Figure 2. (a) schematic of edge cracked specimen (b) actual specimen

### 3.2 Determination of $r_{\max}$ and normalized mode I SIF of the experimental specimen

Material properties from the tensile tests (Table 1) for the PMMA have been used to evaluate the  $r_{\max}$  values for the selected mode I edge cracked experimental specimen (Table 1 and Fig. 2).

Following the numerical approach proposed by Sarangi et al. [12, 13] the  $r_{\max}$  of the experimental edge cracked specimen is found to be 37.0 mm which is indicated in Table 1. Further, using the same FE meshes (that are used for determination of  $r_{\max}$ ) mode I SIF  $K_I$  has been computed. Result of computed normalized SIF,  $F_I$  (Eq. 9) for the selected experimental specimen is also presented in Table 1. All these finite element analyses have been carried using commercial software ANSYS™.

Table 1 Details of different parameters of the edge cracked experimental specimen

| Parameters                  | Values      |
|-----------------------------|-------------|
| $a/b$                       | 0.493       |
| Crack length $a$            | 74 mm       |
| Width $b$                   | 150 mm      |
| Height $h$                  | 114.3 mm    |
| Thickness $t$               | 5.6 mm      |
| Young's modulus $E$         | 2916.91 MPa |
| Poisson's ratio $\nu$       | 0.382       |
| $r_{\max}$                  | 37 mm       |
| Normalized mode I SIF $F_I$ | 2.777738    |

### 3.3 Details of experiment

The selected edge cracked specimen has been loaded in a closed loop servo hydraulic INSTRON 8801 machine with 100 kN capacity under displacement control with an actuator speed 0.1 mm/min. Clevis grips have been used for transferring the tensile load from the machine to the specimen. Strain measurements on the loaded specimens have been carried out using the electrical resistance strain gages of type FLA-1-11-3LT (gage length of 1 mm) and make: TML Japan. The measured strains have been acquired, digitized and processed using NI data acquisition system comprising of cDAQ9178 chassis. Strain measurements have been carried out using NI 9237 (4 channels 24 Bit, half-full bridge analog input module). Experiments have been repeated three times to ensure the repeatability of the results.

## 4. Results and Discussion

Here mode I SIFs have been determined using the DS technique (single strain gage technique) in

order to verify the optimal strain gage locations in mode I specimen and validation of methodology for determination of  $r_{\max}$  (which is useful in deciding optimal locations) proposed by Sarangi et al. [12, 13]. Fig. 2(b) shows the photograph of the edge cracked specimen with  $a/b = 0.493$  and made of PMMA which has been used in the present experiments. Corresponding to Poisson's ratio  $\nu = 0.382$  of the specimen material (Table 1), the orientation of the gage line  $\theta$  is  $53.13^\circ$  (Eq. 4) and the orientation of the gage  $\alpha$  is  $58.28^\circ$ . (Eq. 3).

According to Sarangi et al. [12, 13], the optimal locations for the strain gages should be in the range  $t/2 \leq r \leq r_{\max}$  in order to obtain the accurate value of SIF. Strain gages located beyond the  $r_{\max}$  will result in inaccurate values of SIF  $K_I$  and thus are non-optimal locations. Based on these observations, strain gage locations have been decided in the present experiments as shown in Table 2.

Table 2 Selected radial locations for strain gages

| $r_{\max}$ (mm) | Radial locations |            |               |
|-----------------|------------------|------------|---------------|
|                 | $r_1$ (mm)       | $r_2$ (mm) | $r_3$ (mm)    |
|                 | (Optimal)        | (Optimal)  | (Non-optimal) |
| 37.0            | 17.5             | 35         | 50            |

Fig. 3 show the raw data of measured strain  $\varepsilon_{aa}$  (circled data points) by the strain gages at  $r_1 = 17.5$  mm,  $r_2 = 35$  mm and at  $r_3 = 50$  mm, respectively in a typical test versus the applied load. Fig. 3 also shows best-fit straight lines (solid lines) to the raw data with the corresponding slopes and the correlation coefficients  $R^2$ . As anticipated, at all the strain gage locations, the measured strains are linearly proportional to the applied load as shown by very good values of  $R^2$ . Similar trends with identical values of slopes of best-fit lines and correlation coefficients  $R^2$  have been obtained at all the locations of strain gages in all the three repeated tests.

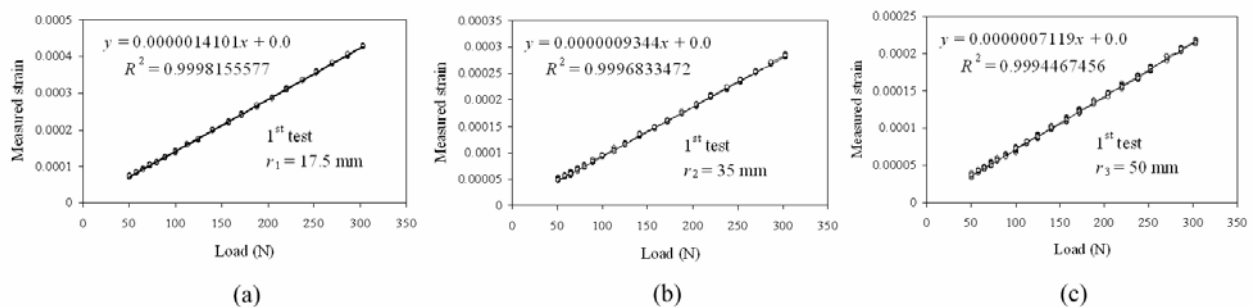


Figure 3. Measured strain versus load (a) at  $r_1 = 17.5$  mm (b) at  $r_2 = 35$  mm and (c) at  $r_3 = 50$  mm

Table 3 shows the experimental values of  $F_I$  obtained at all three gage locations  $r_1, r_2$  and  $r_3$  for each of the three repeated experiments for  $a/b = 0.493$  and their average values. It could be observed that in all the three tests at a given location  $F_I$  values are very close to each other showing the good repeatability of the results.

Table 4 Experimental values of  $F_I$  obtained in all three repeated tests

| Test    | $F_I$                   |                       |                       |
|---------|-------------------------|-----------------------|-----------------------|
|         | $r_1 = 17.5 \text{ mm}$ | $r_2 = 30 \text{ mm}$ | $r_3 = 50 \text{ mm}$ |
| 1       | 2.68641731              | 2.51751109            | 2.29249573            |
| 2       | 2.81463225              | 2.60103297            | 2.38073057            |
| 3       | 2.84759092              | 2.66946702            | 2.53659065            |
| Average | 2.78288016              | 2.59600369            | 2.40327232            |

Table 5 shows the comparison of experimentally determined averaged  $F_I$  values (Table 4) obtained at the optimal and non-optimal locations of strain gages ( $r_1, r_2$  and  $r_3$ ) with the reference solution obtained using ANSYS (Table 1) in terms of the % relative error. The percent relative error in  $F_I$  is determined using Eq. (10).

Table 5 Experimental values of  $F_I$  at different gage locations ( $r_{\max} = 37 \text{ mm}$ )

| Location  | $F_I$                           |                    | % Relative error |
|---|---------------------------------|--------------------|------------------|
|   | Reference solution<br>(Table 1) | Experimental value |                  |
| Optimal<br>( $r_1 = 17.5 \text{ mm} < r_{\max}$ )   |                                 | 2.78288016         | 0.19             |
| Optimal<br>( $r_2 = 35 \text{ mm} < r_{\max}$ )     | 2.777738                        | 2.59600369         | 6.54             |
| Non optimal<br>( $r_3 = 50 \text{ mm} > r_{\max}$ ) |                                 | 2.40327232         | 13.48            |



It is interesting to observe from Table 5 that the % relative error in  $F_I$  is only 0.19% for the strain gage located at the optimal location i.e., at  $r_1 = 17.5 \text{ mm}$  ( $< r_{\max}$ ) while  $F_I$  determined based on the strain gage readings at the non-optimal location  $r_3 = 50 \text{ mm}$  ( $> r_{\max}$ ) is as high as 13.5%. Since the other optimal strain gage location  $r_2 = 35 \text{ mm}$  which is very close to  $r_{\max}$ , slightly more error can be noticed at this location as compared to the gage location at  $r_1$ . However, this error is still within the acceptable limits. These experimental observations clearly verify the existence of optimal gage locations and their use in determination of accurate values of mode I SIFs. It should be noted that these optimal and non-optimal gage locations have been decided based on the Eq. (6) for which  $r_{\max}$  is required for a configuration. Thus, the experimental results in Table 5 also substantiate the efficacy of methodology proposed by Sarangi et al. [12, 13] for determination  $r_{\max}$  and its importance in deciding the optimal strain gage locations for accurate determination of mode I SIF. Moreover, the results in Table 5 clearly show the importance of  $r_{\max}$  for selection of optimal strain gage locations.

## 5. Conclusions

The present investigation examines the experimental verification of optimal strain gage locations and their importance in accurate determination of mode I SIFs. This examination also validates the methodology for determination of maximum permissible strain gage radial location  $r_{\max}$  proposed by Sarangi et al. [12, 13] and its use in locating the optimal strain gage locations for accurate determination of SIFs using the DS technique. The results of the present investigation clearly demonstrate that very accurate mode I SIFs can be determined using the DS technique if the strain gages are placed within the  $r_{\max}$  value i.e., optimal locations. The results also show that the experimentally obtained SIFs using the strain gages placed at non-optimal locations (i.e., beyond  $r_{\max}$  value of a specimen) contain significant errors.

### Acknowledgements

Authors gratefully acknowledge financial support from the Naval Research Board (NRB), Ministry of Defence, India, under grant number NRB-167/MAT/08-09.

### References

- [1] K. Ravi-Chandar, Fracture Mechanics, in: W.N. Jr. Sharpe (Ed.), Springer Handbook of Experimental Solid Mechanics, Springer Science + Business Media, New York, 2008, pp. 125-158.
- [2] J.W. Dally, R.H. Sanford, Strain gage methods for measuring the opening mode stress intensity factor. *Exp Mech*, 27 (1987) 381–388.
- [3] J.H. Kuang, L.S. Chen, A single strain gage method for  $K_I$  measurement. *Eng Fract Mech*, 51 (1995) 871–878.
- [4] J. Wei, J.H. Zhao, A two-strain-gage technique for determining mode I stress-intensity factor. *Theor Appl Fract Mech*, 28 (1997) 135–140.
- [5] J.W. Dally, D.B. Barker, Dynamic measurements of initiation toughness at high loading rates. *Exp Mech*, 28 (1988) 298–303.
- [6] A. Shukla, B.D. Agarwal, B. Bhushan, Determination of stress intensity factor in orthotropic composite materials using strain gages. *Eng Fract Mech*, 32 (1989) 469–477.
- [7] L. Parnas, O.G. Bilir, Strain gage methods for measurement of opening stress intensity factor. *Eng Fract Mech*, 55 (1996) 485–492.
- [8] S. Rijal, H. Homma, Dimple fracture under short pulse loading. *Int J Impact Eng*, 24 (2000) 69-83.
- [9] J.F. Kalthoff, A. Burgel, Influence of loading rate on shear fracture toughness for failure mode transition. *Int J Impact Eng*, 30 (2004) 957-971.
- [10] S. Shirley, H. Homma, Approach to dynamic fracture toughness of GFRP from aspect of viscoelastic and debonding behaviors. *J Solid Mech Mat Eng*, 1 (2007) 275-286.
- [11] S. Swamy, M.V. Srikanth, K.S.R.K. Murthy, P.S. Robi, Determination of the mode I stress intensity factors of the complex configurations using the strain gages. *J Mech Mater Struct*, 3 (2008) 1239–1255.
- [12] H. Sarangi, K.S.R.K. Murthy, D. Chakraborty, Radial locations of strain gages for accurate measurement of mode I stress intensity factor. *Mater Des*, 31 (2010) 2840-2850.
- [13] H. Sarangi, K.S.R.K. Murthy, D. Chakraborty, Optimum Strain gage location for evaluating stress intensity factors in single and double ended cracked Configurations. *Eng Fract Mech*, 77 (2010) 3190-3203.
- [14] W. Yang, L.B. Freund, Transverse shear effects for through-cracks in an elastic plate. *Int J Solids Struct*, 21 (1985) 977-994.
- [15] J. Rosakis, K. Ravi-Chandar, On crack-tip stress state: An experimental evaluation of three-dimensional effects. *Int J Solids Struct*, 22 (1986) 121–134.
- [16] T.M. Maccagno, J.F. Knott, The fracture behaviour of PMMA in mixed modes I and II. *Eng Fract Mech*, 34 (1989) 65-68.